

## Influence of the dendron chemical structure on the photophysical properties of bisfluorene-cored dendrimers

J. C. Ribierre,<sup>1</sup> A. Ruseckas,<sup>1</sup> I. D. W. Samuel,<sup>1,a)</sup> H. S. Barcena,<sup>2,3</sup> and P. L. Burn<sup>2,3</sup>

<sup>1</sup>*Organic Semiconductor Centre, SUPA, School of Physics and Astronomy, University of St. Andrews, North Haugh, St. Andrews, Fife KY16 9SS, United Kingdom*

<sup>2</sup>*Department of Chemistry, Chemistry Research Laboratory, University of Oxford, Mansfield Road, OX1 3TA Oxford, United Kingdom*

<sup>3</sup>*Centre for Organic Photonics and Electronics, Chemistry Building, University of Queensland, Queensland, 4072, Australia*

(Received 26 November 2007; accepted 11 April 2008; published online 27 May 2008)

A detailed study of the photophysics of a family of bisfluorene-cored dendrimers is reported. Polarized time-resolved fluorescence, singlet-singlet exciton annihilation and fluorescence quantum yield measurements were performed and used to understand how the dendron structure affects the light-emitting properties of the materials. The exciton diffusion rate is similar in all films studied. An increase in the nonradiative deactivation rate by nearly one order of magnitude is observed in films of dendrimers with stilbenyl and carbazolyl based dendrons as compared to solutions, whereas the dendrimers with biphenyl and diphenylethylenyl dendrons showed highly efficient emission (photoluminescence quantum yields of 90%) in both solution and the solid state. The results of the materials that show fluorescence quenching can be explained by the presence of quenching sites at a concentration of just a fraction of a percent of all macromolecules. A possible explanation of this quenching is hole transfer from the emissive chromophore to the dendron in a face-to-face geometry. These results are important for the design of efficient blue emitters for optoelectronic applications. © 2008 American Institute of Physics. [DOI: 10.1063/1.2919567]

### I. INTRODUCTION

Organic semiconductors have received a great deal of attention due to their high potential for applications in optoelectronic devices including organic light-emitting diodes (OLEDs),<sup>1–3</sup> photovoltaics,<sup>4,5</sup> and field-effect transistors.<sup>6,7</sup> These materials can be divided into three main categories: small molecules, which are normally evaporated under vacuum to form thin films, solution-processed polymers, and dendrimers. The photoluminescence (PL) and electrical properties of conjugated polymers as well as the device performance are strongly influenced by the film's morphology, which depends on the conformation of the polymer chains and interchain interactions.<sup>8–17</sup> To some extent, these can be controlled by the choice of the processing solvent, the solution concentration, the spin-coating conditions, and thermal annealing.<sup>9–15</sup> However, conjugated polymers have a distribution of molecular weights, and hence chain lengths as well as considerable conformational disorder,<sup>8,18–21</sup> which can complicate the development of structure-property relationships.

Light-emitting dendrimers are macromolecules with a well-defined structure and are composed of a core, dendrons, and surface groups. The appropriate selection of each of these components provides a good and independent control of the electronic and solution processing properties. This makes them convenient model systems in which to study organic semiconductor physics.<sup>22–24</sup> It also facilitates the de-

velopment of materials combining favorable optoelectronic and processing properties leading to, for example, highly efficient phosphorescent LEDs with external quantum efficiencies of as high as 16%.<sup>25</sup> Film morphology is a key area for all organic semiconductors and is still unexplored in light-emitting dendrimers. Different aspects of the dendrimer materials can affect the molecular packing of the dendrimer in thin films: the dendron type, the dendron generation, the number of dendrons, and the dendrimer shape. In order to improve our understanding of the structure-property relationships in conjugated dendrimers, it is now critical to establish the influence of the molecular structure on the intermolecular interactions and the optoelectronic properties of these materials.

In this manuscript, we investigate the influence of the dendron chemical structure on the photophysical properties and the exciton diffusion of first-generation fluorescent bisfluorene-cored dendrimers. Such dendrimers have been successfully used to make deep blue OLEDs,<sup>26</sup> one-<sup>27</sup> and two-photon<sup>28</sup> pumped lasers, and optical amplifiers.<sup>29</sup> The different dendrons attached to the 7-positions of the 9,9-di-*n*-hexylfluorenyl groups making up the bisfluorene core are shown in Fig. 1 and are as follows: biphenyl (BP), biphenylcarbazolyl (BPCz), *E*-stilbenyl (ES), and diphenylethylenyl (DPE). 2-ethylhexyloxy surface groups were used for all the dendrimers. The “molecular groups” in the dendrons show different geometries and rigidity, give different shapes to the dendrimer, and modify the packing of the dendrimers in thin films. The variations observed in the optical spectra, PL quantum yield (PLQY), and PL kinetics of the

<sup>a)</sup>Electronic mail: idws@st-andrews.ac.uk.

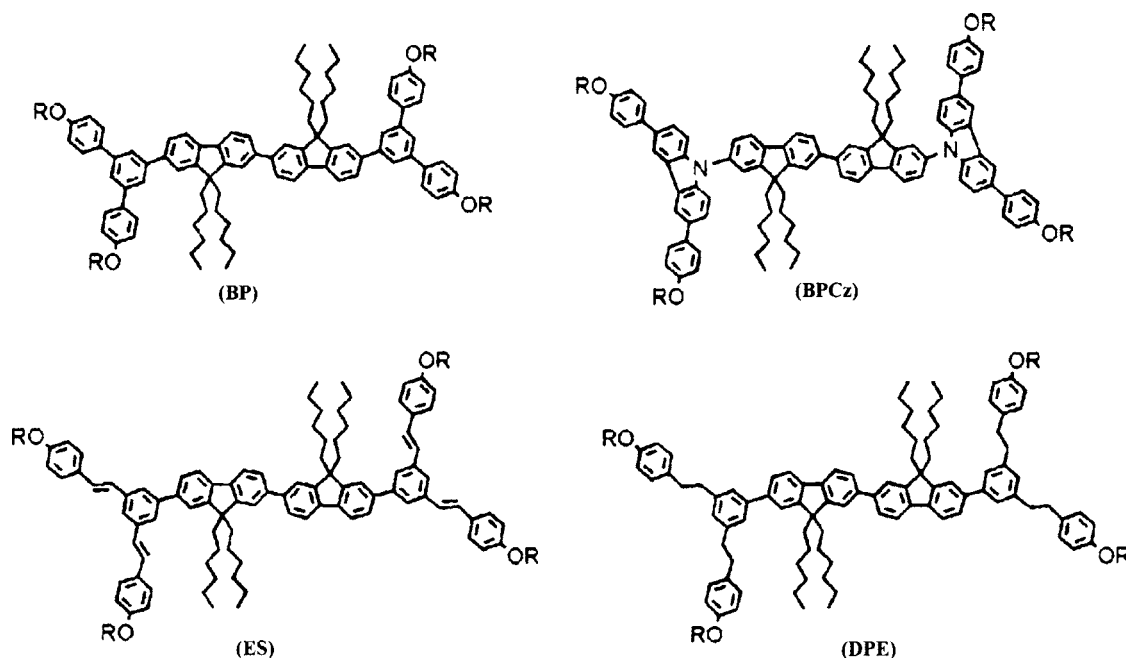


FIG. 1. Chemical structures of the four dendrimers used in this study.  $R=2$ -ethylhexyl.

four dendrimers are attributed to changes in the intermolecular interactions and the concentration quenching effects. In contrast, exciton diffusion studied by both exciton-exciton annihilation and fluorescence depolarization measurements is independent of the dendron type. Modeling the concentration quenching as energy transfer of the excitons to quenching sites shows the effects of the dendrons on the concentration of quenchers. While no quenchers are present in the neat films of bisfluorene with BP and DPE dendrons, we found one quenching site per 370 molecules of the dendrimers with BPCz dendrons and per 500 of those with ES dendrons. A possible explanation of the observed fluorescence quenching is the charge transfer from the bisfluorene cores to the ES and BPCz dendrons. These results clarify the role of the dendron type on the intermolecular interactions and provide new insights in the photophysics of light-emitting dendrimers.

## II. EXPERIMENT

Samples for solution measurements were prepared by dissolving the dendrimers in tetrahydrofuran and degassing by three freeze-pump-thaw cycles before measurements. The typical concentration of these solutions was around  $2 \times 10^{-6} M$ . Thin films were made from a chloroform solution by spin coating onto precleaned fused silica substrates. The solution concentration was 20 mg/ml and the spin speed was 1000 rpm for 1 min. The thickness of these thin films was determined from spectroscopic ellipsometry and was between 170 and 190 nm.

Absorption and PL spectra were recorded on a Cary Varian model 300 absorption spectrophotometer and a Jobin Yvon Fluoromax 2 fluorimeter, respectively. The solution PLQY value was determined with the use of quinine sulfate in 0.5M sulfuric acid (PLQY of 51%) as a reference.<sup>30</sup> The excitation wavelength was 360 nm and the absorbance of the

solutions was around 0.1. The PLQY of the films was determined by using an integrating sphere purged with flowing nitrogen and a helium-cadmium laser with a wavelength of 325 nm and a power of 0.15 mW.<sup>31</sup> For the time-resolved PL measurements, samples were excited by 100 fs pulses at 400 nm with a repetition rate of either 50 kHz or 80 MHz. Time-resolved PL integrated over the spectral range of 410–540 nm was recorded by a synchroscan streak camera with an instrumental response function of 2 ps. All these PL measurements were performed at room temperature and the films were placed in a vacuum of  $<5 \times 10^{-4}$  mbar. For the time-resolved fluorescence anisotropy measurements, the PL intensities  $I_{\text{par}}(t)$  and  $I_{\text{per}}(t)$  for the fluorescence polarized parallel and perpendicular to the excitation polarization, respectively, were measured and the fluorescence anisotropy  $r$  was calculated by using the following equation:  $r = (I_{\text{par}}(t) - GI_{\text{per}}(t)) / (I_{\text{par}}(t) + 2GI_{\text{per}}(t))$ , where  $G$  is a detection sensitivity correction factor, which was applied by tail matching of  $I_{\text{par}}(t)$  and  $I_{\text{per}}(t)$ , assuming a full depolarization of fluorescence during its lifetime. For the exciton-exciton annihilation measurements, 50 kHz excitation pulses were used and the spot size was determined by a beam profiler and showed a diameter of 160  $\mu\text{m}$  at  $1/e^2$  of the maximum intensity. The excitation density was varied by neutral density filters and estimated from the energy density of the absorbed light pulse.

The electrochemical measurements of the bisfluorene-cored dendrimers and their dendrons in dry dichloromethane were carried out in a standard three-electrode cell, using platinum as working and counterelectrodes and Ag/AgNO<sub>3</sub> in acetonitrile as the reference electrode. The electrochemical potentials were calibrated by reference to the ferricenium/ferrocene/ferrocenium couple with  $E_{1/2} = 0.135$  V. The  $E_{1/2}$ s of the dendrimers were determined from cyclic voltammograms collected at a scan rate of 1000 mV/s. The ionization

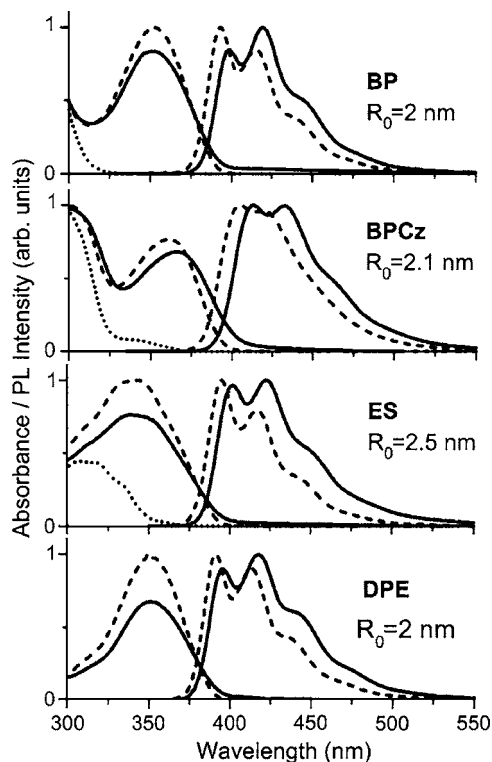


FIG. 2. The absorption and PL spectra of the bisfluorene-cored dendrimers in solution (dashed line) and in neat film (solid line). The absorption spectra of the dendrons in solution are also shown (dotted line). The values of the Förster radius  $R_0$  determined from the spectra in solution using Eq. (2) are given in the insets.

potentials were calculated from the  $E_{1/2s}$  by comparison with 4,4'-bis(*N*-3-methylphenyl-*N*-phenyl)biphenyl for which both the oxidation and ionization potential are known.<sup>32</sup> The electron affinity was then calculated by combining the values of the ionization potential and the optical bandgap estimated from the peak position of the long wavelength absorption in the spectra measured in solution. It has been previously found in conjugated dendrimers that the electrochemical bandgap could match the peak of the optical absorption.<sup>33</sup>

### III. RESULTS AND DISCUSSION

#### A. Steady-state absorption and PL spectra

Figure 2 shows the absorption of the dendrimers in solution and in the solid state. The absorption feature at 350 nm is due to the chromophore comprised of the bisfluorene core and the first branching group of each of the dendrons for all materials. The BP and DPE dendrons absorb in the deep UV ( $\lambda < 320$  nm), while the BPCz and ES dendrons show absorption between 300 and 380 nm,<sup>34</sup> which also contributes to the long wavelength absorption spectra of these two dendrimers. The absorption spectra in solution also show that these materials are fully transparent in the visible region. In the case of thin films, the long tails at wavelengths higher than 400 nm are attributed to the changes in the refractive index of the dendrimer films.

The influence of the dendrons on the emission spectra was also investigated. As depicted in Fig. 2, the PL spectra of the dendrimers in solution present a similar shape with two vibronic peaks and one shoulder. Table I gives the position of the PL 0-0 peaks, which are found to be very similar for the dendrimers with BP, ES, and DPE dendrons. In contrast, the PL spectrum of the bisfluorene-cored dendrimer with BPCz dendrons is  $\sim 10$  nm redshifted and has a less well-defined vibronic structure. A similar redshift is observed in the absorption peak of this material and is attributed to the presence of the carbazole moieties. For all the bisfluorene-cored dendrimers studied, the PL spectra measured in thin films are 5–8 nm redshifted compared to those measured in solution and this shift is slightly more pronounced in the case of dendrimers with BPCz and ES dendrons, as summarized in Table I.

It can also be noticed from Fig. 2 that there is an overlap of the absorption and the PL spectra of the dendrimers. This suggests that the singlet excitons can migrate in these materials by a Förster type dipole-dipole coupling.<sup>35</sup> The energy transfer rate  $k_{ET}$  according to that mechanism is inversely proportional to the sixth power of the distance  $R$  between molecules as expressed in the following expression:

TABLE I. Position of the PL 0-0 vibronic peak, quantum yield (PLQY), lifetime ( $\tau$ ), radiative ( $k_R$ ), and nonradiative ( $k_{NR}$ ) decay rates of the  $S_1$  state. The uncertainties of  $k_R$  are  $\pm 5\%$  determined by the accuracy of the PLQY measurements. The values of the ionization potential ( $I_p$ ) and the electron affinity ( $E_a$ ) are relative to the vacuum level.

|                 | $\lambda_{0-0}$<br>(nm) | PLQY<br>(%)     | $\tau$<br>(ns) | $k_R$<br>( $\times 10^9$ s $^{-1}$ ) | $k_{NR}$<br>( $\times 10^9$ s $^{-1}$ ) | $I_p$<br>(eV) | $E_a$<br>(eV) |
|-----------------|-------------------------|-----------------|----------------|--------------------------------------|---|---------------|---------------|
| BP (solution)   | 392                     | 93              | 0.73           | 1.3                                  | 0.1                                     | 6.2           | 2.6           |
| (film)          | 397                     | 92 <sup>a</sup> | 0.73           | 1.3                                  | 0.1                                     |               |               |
| BPCz (solution) | 405                     | 89              | 1.4            | 0.6                                  | 0.1                                     | 5.9           | 2.5           |
| (film)          | 413                     | 43 <sup>a</sup> | 0.7            | 0.6                                  | 0.8                                     |               |               |
| (dendrion)      | 371                     | 20              | 4              | 0.05                                 | 0.2                                     | 5.8           | 2.2           |
| ES (solution)   | 395                     | 90              | 0.83           | 1.1                                  | 0.1                                     | 6.3           | 2.7           |
| (film)          | 402                     | 52 <sup>a</sup> | 0.48           | 1.1                                  | 1                                       |               |               |
| (dendrion)      | 368                     | 12              | 0.64           | 0.2                                  | 1.4                                     | 6.0           | 2.4           |
| DPE (solution)  | 391                     | 90              | 0.72           | 1.25                                 | 0.1                                     | 6.2           | 2.6           |
| (film)          | 396                     | 89              | 0.73           | 1.25                                 | 0.1                                     |               |               |

<sup>a</sup>These values have been previously reported in Ref. 27.

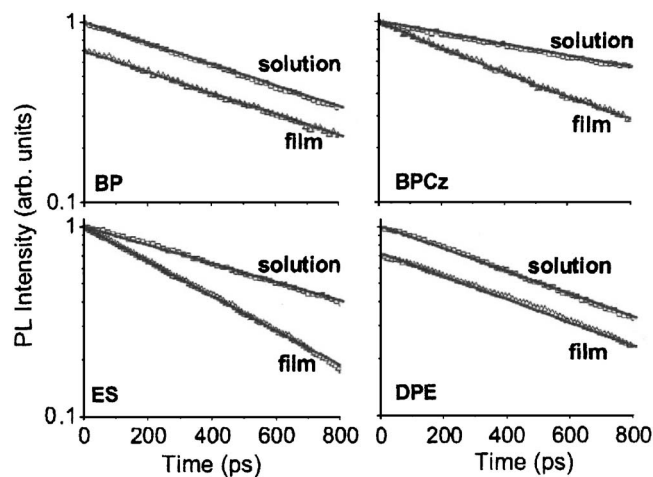


FIG. 3. PL decays of the bisfluorene-cored dendrimers in solution and in the solid state. The solid lines are the fits to the data obtained from a single exponential decay function.

$$k_{\text{ET}} = \frac{1}{\tau} \left( \frac{R_0}{R} \right)^6, \quad (1)$$

where  $\tau$  is the PL lifetime and  $R_0$  is the Förster radius, which corresponds to the critical transfer distance over which the rate of de-excitation of the donor due to the fact that energy transfer is equal to that associated with radiative decay.  $R_0$  can be found from the overlap between the molar extinction coefficient  $\varepsilon_A(\lambda)$  and the normalized PL spectra  $F_D(\lambda)$  of the dendrimers by<sup>35</sup>

$$R_0^6 = \frac{9000 \ln 10 \kappa^2 \text{PLQY}}{128 \pi^5 n^4 N_A} \int_0^\infty F_D(\lambda) \varepsilon_A(\lambda) \lambda^4 d\lambda, \quad (2)$$

where  $\kappa$  is the orientational factor equal to  $2/3$  in the case of random directional distribution for the donor and acceptor molecules,  $N_A$  is Avogadro's number, and  $n$  is the refractive index. We have calculated  $R_0$  from the absorption and PL spectra measured in solution and the values for each dendrimer are listed in the insets of Fig. 2. We found  $R_0$  values of 2.1 and 2.5 nm for the dendrimers with BPCz and ES dendrons, respectively, which is slightly larger than that of 2 nm calculated for the molecules with BP and DPE dendrons. We are not able to calculate  $R_0$  in films because of the long tails on the spectra above 400 nm associated with reflection and scattering losses, so we use the solution value as an estimate of  $R_0$  in films.

## B. Fluorescence lifetime and quantum yield

Figure 3 shows the PL kinetics of the bisfluorene-cored dendrimers measured in both solution and thin film. These PL decays are independent of both the emission wavelength across the overall PL spectra and the excitation wavelengths (266, 375, and 400 nm), which suggest that excitons formed on the dendrons are rapidly transferred to the emissive chromophore. A single exponential decay function can be used to fit the decays with a characteristic PL lifetime  $\tau$ , which is given in Table I. All the materials show a similar PLQY of around 90% in solution but different PL lifetimes. Whereas the dendrimers with BP and DPE dendrons exhibit a PL life-

time of 0.73 ns, dendrimers with BPCz and ES dendrons show longer PL lifetimes of 1.4 and 0.83 ns, respectively. From the determination of the PLQY and the PL lifetime, we calculate the radiative and nonradiative decay rates, denoted as  $k_R$  and  $k_{NR}$ , respectively, by using the following expressions:

$$\text{PLQY} = \frac{k_R}{k_R + k_{NR}}, \quad \tau = \frac{1}{k_R + k_{NR}}. \quad (3)$$

The values of  $k_R$  and  $k_{NR}$  obtained by using Eq. (3) are listed in Table I. The radiative decay rate was found to be about  $1.25 \times 10^9 \text{ s}^{-1}$  for the dendrimers with BP and DPE dendrons, while the rate for the dendrimer with the ES dendrons was slightly lower. These values are consistent with the radiative decay rate of  $1.2 \times 10^9 \text{ s}^{-1}$  reported in terfluorene.<sup>36</sup> The radiative decay rate of the dendrimer with the BPCz dendrons was smaller by a factor of 2. The emitting chromophore in BP, ES, and DPE is composed of the bisfluorene core and the first phenyl ring of each of the dendrons. The small effect of ES dendrons on  $k_R$  could be due to inductive effects or local dielectric changes. In the case of the dendrimer with BPCz dendrons, the decrease in  $k_R$  indicates that conjugation with carbazole groups significantly decreases the fluorescence decay rate.

Figure 3 also shows that the PL kinetics and the PLQY measured in the dendrimers with BP and DPE dendrons are the same in solution and in thin film, which indicates the absence of additional PL quenching in the solid state. This makes these materials extremely efficient solid state light emitters, and it is interesting that this can be achieved with only a first-generation dendrimer. In contrast, the PL kinetics become faster and the PL quantum yield strongly decreases in the solid state for the dendrimers with BPCz and ES dendrons. While the radiative decay rate is unchanged from solution, the nonradiative decay rate is much higher in the solid state for these two dendrimers. These results illustrate the important role that can be played by the dendrons in controlling PL quenching.

## C. Excitation energy transfer in films

To understand this increase in the nonradiative deactivation rate in films of dendrimers with BPCz and ES dendrons, we studied exciton diffusion. Two methods were used: fluorescence depolarization and exciton-exciton annihilation. Figure 4 shows the fluorescence anisotropy decays measured in neat films of all four dendrimers. The values of their initial anisotropy range from 0.3 to 0.35, which is close to the theoretical value of 0.4 for randomly oriented noninteracting chromophores. Their kinetics can be described by  $r = r_0 \exp[(-t/\tau_{\text{dep}})^{1/2}]$ , with the depolarization time  $\tau_{\text{dep}}$  listed in Table II. This method follows theoretical and experimental studies of exciton diffusion via Förster energy transfer in an ensemble of randomly oriented chromophores.<sup>37</sup> The singlet excitons diffuse in these materials by incoherent hopping and there is some loss of polarization memory with each hop. Dendrimers are not expected to pack with any significant short range order, therefore, a single hop is sufficient to cause a loss of polarisation by a factor of  $1/e$  and an average

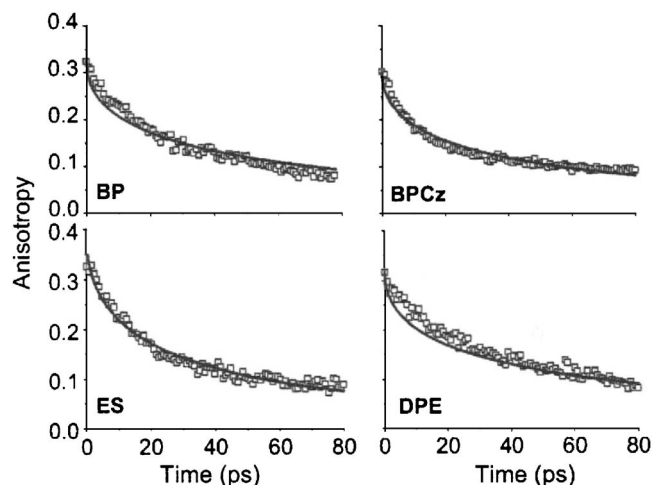


FIG. 4. Fluorescence depolarization of the bisfluorene-cored dendrimer neat films. Solid lines are the fits obtained with a stretched exponential decay function as described in the text.

hopping rate can be estimated as  $k_h = 1/\tau_{\text{dep}}$ . In the case of incoherent hopping in three dimensions,  $k_h$  is related to the exciton diffusion coefficient  $D$  by<sup>38</sup>  $D = R^2 k_h / 3$ , where  $R$  is the distance between the two nearest neighbors. This distance  $R$  was calculated assuming a film density of  $1 \text{ g/cm}^3$  and the dendrimers are hard spheres. The values of  $D_{\text{depolarization}}$  are listed in Table II and are found around  $(2.4 \pm 0.4) \times 10^{-4} \text{ cm}^2 \text{ s}^{-1}$ . This value is much lower than that of  $2 \times 10^{-2} \text{ cm}^2 \text{ s}^{-1}$  previously reported in polyfluorenes,<sup>39</sup> suggesting that dendrons slow down the exciton diffusion. This is a useful attribute in a number of situations: it reduces exciton-exciton annihilation in lasers (and LEDs), it reduces the impact of any quenching sites in a material, and it helps excitons to remain in the layer in which they are generated in LEDs. Values of  $D$  are very similar in all four dendrimers, implying a similar strength of dipole-dipole interactions between the emissive chromophores in these materials.

Exciton-exciton annihilation measurements are another experimental technique employed to study exciton diffusion in organic thin films.<sup>40,41</sup> It occurs at high excitation densities (typically  $> 10^{17} \text{ cm}^{-3}$ ) when two excitons collide to form a single higher excited state, leading to the loss of one exciton as heat. Figure 5(a) shows that the PL decays measured at various excitation densities in a neat film of the dendrimer with BPCz dendrons become nonexponential and is much

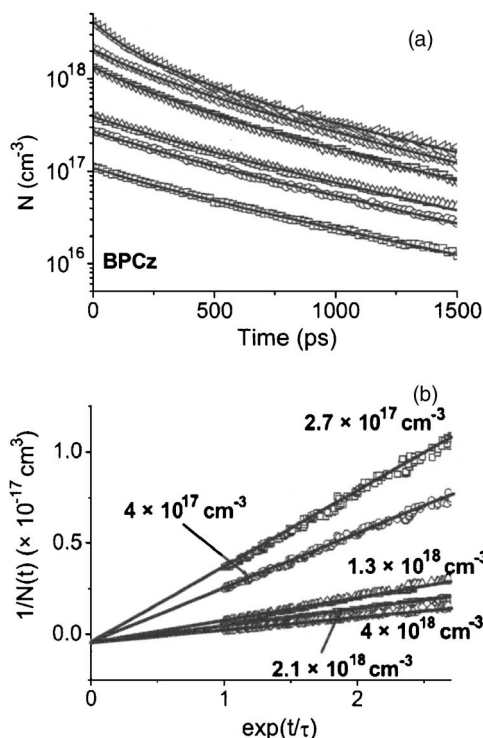


FIG. 5. (a) PL decays of the dendrimer with BPCz dendrons in the neat film measured at various excitation densities. Solid lines are the fits obtained using Eq. (5). (b) Plots of the inverse of the exciton density in neat film of the dendrimer with BPCz dendrons against  $\exp(t/\tau)$  at several excitation densities. Solid lines are the fits obtained by using Eq. (7).

faster for excitation densities higher than  $2 \times 10^{17} \text{ cm}^{-3}$ . Similar behavior was observed in the other bisfluorene-cored dendrimers. The density of excitons  $N(t)$  as a function of time, which is proportional to the PL intensity, can be described by the following rate equation:

$$\frac{d}{dt}N(t) = G(t) - \frac{1}{\tau}N(t) - \gamma N^2(t), \quad (4)$$

where  $\tau$  is the PL lifetime in the absence of annihilation and  $\gamma$  is the annihilation rate constant.  $G(t)$  is the exciton generation rate, which can be approximated as a  $\delta(t)$  function since it is very fast and is limited by the time resolution of the streak camera which is around 2 ps. In this case, the solution of Eq. (4) for the time independent  $\gamma$  is

TABLE II. Summary of the exciton diffusion data obtained in the dendrimer neat films. The average center-to-center distance  $R$  between molecules is calculated by using a density of  $1 \text{ g/cm}^3$ ,  $\tau_{\text{dep}}$  is the time constant describing the dynamics of the fluorescence depolarization,  $\gamma$  is the exciton-exciton annihilation constant,  $D_{\text{depolarization}}$  and  $D_{\text{annihilation}}$  are the diffusion constants found, respectively, by fluorescence depolarization and annihilation measurements, and  $N_q/N_0$  is the ratio between the concentration of quenchers  $N_q$ , and the concentration of dendrimers in the films  $N_0$ .

| Dendrion type | $R$ (nm) | $\tau_{\text{dep}}$ (ps) | $D_{\text{depolarization}}$ ( $\times 10^{-4} \text{ cm}^2 \text{ s}^{-1}$ ) | $\gamma$ ( $\times 10^{-10} \text{ cm}^3 \text{ s}^{-1}$ ) | $D_{\text{annihilation}}$ ( $\times 10^{-4} \text{ cm}^2 \text{ s}^{-1}$ ) | $N_q/N_0$ |
|---------------|----------|--------------------------|--|--|--|-----------|
| BP            | 1.73     | 50                       | 2.0  | 4.5  | 2.1  |           |
| BPCz          | 1.79     | 40                       | 2.6  | 6.1  | 2.7  | 1/370     |
| ES            | 1.77     | 40                       | 2.6  | 5.7  | 2.5  | 1/500     |
| DPE           | 1.77     | 50                       | 2.1  |  |  |           |

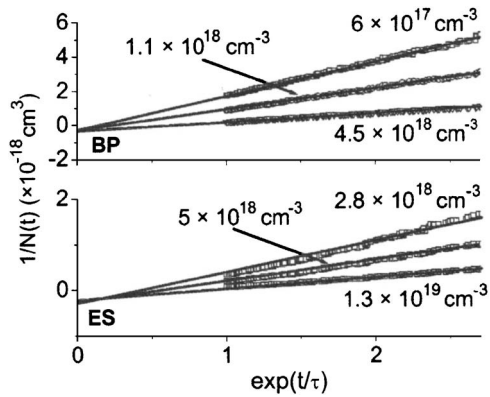


FIG. 6. Plots of the inverse of the exciton density in neat film of the dendrimer with BP and ES dendrons against  $\exp(t/\tau)$  at several excitation densities. Solid lines are the fits obtained by using Eq. (7).

$$N(t) = \frac{N_0 \exp(-t/\tau)}{1 + \gamma\tau N_0 [1 - \exp(-t/\tau)]}, \quad (5)$$

where  $N_0$  is the initial exciton density immediately after the pulse excitation and is calculated by using the following equation:

$$N_0 = \frac{4 \lambda P (1 - 10^{-A})}{\pi d^2 h c f L}, \quad (6)$$

where  $P$  is the average excitation power,  $A$  is the absorbance of the film at the wavelength of the excitation light  $\lambda$ ,  $d$  is the diameter of the excitation spot,  $L$  is the film thickness,  $h$  the Planck constant,  $c$  is the light velocity, and  $f$  is the repetition rate of the excitation laser pulses. Equation (5) can be rewritten as

$$\frac{1}{N(t)} = \left[ \frac{1}{N_0} + \gamma\tau \right] \exp(t/\tau) - \gamma\tau. \quad (7)$$

The inverse of the exciton density is expected to vary linearly as a function of  $\exp(t/\tau)$  with a slope and an intercept with the  $y$  axis depending on the annihilation constant  $\gamma$ . The solid lines in Figs. 5(b) and 6 were calculated using Eq. (7). The best fits were obtained with  $\gamma = 4.5 \times 10^{-10} \text{ cm}^3 \text{ s}^{-1}$  for the dendrimer with BP,  $\gamma = 6.1 \times 10^{-10} \text{ cm}^3 \text{ s}^{-1}$  for the dendrimer with BPCz, and  $\gamma = 5.7 \times 10^{-10} \text{ cm}^3 \text{ s}^{-1}$  for the dendrimer with ES dendrons. As the singlet-singlet annihilation process removes one exciton per interaction, the appropriate relation for our  $\gamma$  values to the diffusion constant  $D$  in the case of diffusion limited annihilation is

$$\gamma = 4\pi R_a D, \quad (8)$$

where  $R_a$  is the annihilation radius of excitons, which corresponds to the distance over which annihilation is faster than diffusion. The  $D_{\text{annihilation}}$  values are obtained by taking  $R_a$  as  $R$  the average spacing between the centers of the two nearest neighboring bisfluorene cores. As shown in Table II, they are very consistent with the data obtained from fluorescence depolarization. This confirms that the migration of singlet excitons in bisfluorene-cored dendrimers is weakly affected by the dendron type.

## D. Nature of fluorescence quenching

The lower PLQY of some materials in the thin film is due to an increased nonradiative decay and we attribute this to excitation transfer to quenching sites. In the case of infinite capture rate at a distance  $R$  from the quencher, the quenching dynamics can be described by the rate constant  $k_q$  defined as<sup>42</sup>

$$k_q(t) = 4\pi D R N_q \left( 1 + \frac{R}{\sqrt{Dt}} \right), \quad (9)$$

where  $N_q$  is the concentration of quenchers. The PL kinetics of BPCz and ES in the neat films can be fitted by an exponential decay with a rate  $k = k_R + k_{\text{NR-}i} + k_q(t)$ , where  $k_{\text{NR-}i}$  corresponds to the nonradiative decay rate of isolated molecules and is assumed here to be equal to the decay rate measured in solution. Taking  $R$  as the core-core average spacing distance (center to center) and the values of  $D$  determined from annihilation measurements, we obtained  $N_q/N_0$  equal to 1/370 and 1/500 in BPCz and ES, respectively (see Table II), where  $N_0$  is the concentration of dendrimers in the neat films. In contrast, materials with BP and DPE dendrons show no detectable PL quenching even though the exciton diffusion rate and thus intermolecular dipole-dipole interactions are similar in all dendrimers. This suggests that quenchers are specific to the BPCz and ES dendrons. Chemical defects arising from synthesis techniques could cause low numbers of quenchers but the dendrimers have the advantage over polymers in that they are much easier to purify and that there are no end groups. A missing dendron or component of a dendron can make a big difference to the polarity of the material, enabling it to be separated, unlike the difference one monomer makes in polymer. The quenchers are also unlikely to be excimers because we did not observe any changes in the PL spectra and also we did not observe any spectral dependence of the fluorescence lifetime. The exciton lifetime in bisfluorene films with BPCz and ES dendrons decreases by a factor of 2 as compared to solutions; therefore, if excimers are involved, about 50% of excitations would end up on a quenching site and would show some excimer emission. Energy transfer from the emissive chromophore to the BPCz or ES dendrons followed by a fast nonradiative deactivation of the excited state has to be considered as a possible quenching mechanism. However, as depicted in Fig. 7, the PL spectra of these dendrons are more than 25 nm blueshifted with respect to those measured for the dendrimers, which makes the up-hill energy transfer to dendrons inefficient. In addition, the PL lifetime of 4 ns measured in the BPCz dendron is by a factor of 3 longer than that of the dendrimer itself, so that a fast decay on the dendron can be excluded. We note that a slightly shorter PL lifetime of 0.64 ns in the Br-substituted ES dendron can be explained by an enhanced intersystem crossing rate due to a ‘‘heavy atom’’ effect. On the basis of these arguments, we exclude quenching by energy transfer to dendrons.

Charge transfer between the core and the dendrons is the most plausible mechanism of PL quenching and is consistent with the electrochemistry data summarized in Table I. However, it is difficult to provide conclusive evidence that a type

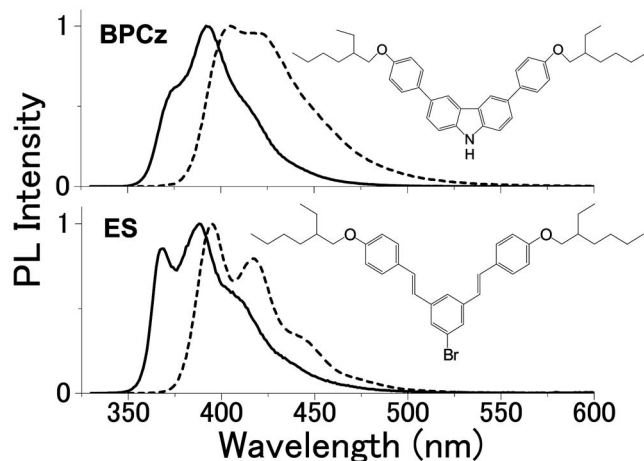


FIG. 7. PL spectra of the BPCz and ES dendrimers (dashed lines) and their dendrons (solid lines). The excitation wavelength was 325 nm. The chemical structures of the dendrons are shown in the insets.

II heterojunction is formed between the ES and BPCz dendrons because the oxidation potentials of the dendrons and emissive chromophores cannot be separated. It is worth noting that the exciton binding energy in bisfluorene is at least as high as that in polyfluorene,<sup>43</sup> which is about 1 eV. The energy offset of the highest occupied molecular orbital levels is very small, therefore, hole transfer can only occur if the Coulombic energy of the separated electron-hole pair was at least 0.9 eV, which corresponds to a separation distance of about 5 Å for  $\epsilon=3$ , typical for organic semiconductors. This short distance requires a face-to-face geometry ( $\pi$ - $\pi$  stacking) of the bisfluorene core and the dendron, which is only possible between separate molecules because the single bond linkage does not allow folding of the dendron onto the core.

From the exciton diffusion results, the quenchers in films are confined to few sites (concentration up to 0.3% of all dendrimers). Their low concentration can be explained by the dendrimer structure which tends to reduce intermolecular interactions and to inhibit  $\pi$ - $\pi$  stacking. It is worth noting that we observed a strong thickness dependence of the PL decays (data not shown) in ES dendrimer neat films, which suggests that the concentration of quenchers and the molecular stacking might change with the film thickness. Our results suggest that quenching is due to charge transfer to the dendrons and point out the importance of the dendron chemical structure on the intermolecular interactions and the photophysical properties of bisfluorene-cored dendrimers. This study should be taken into account in the further development of efficient blue fluorescent or phosphorescent dendrimers with charge transporting dendrons for light-emitting applications.

#### IV. CONCLUSIONS

We have performed PL measurements on a series of bisfluorene-cored dendrimers to study the influence of the dendron chemical structure on the excitation migration and the concentration quenching observed in some of these materials. Our experiments demonstrate a significant dependence of the optical spectra, photoluminescence quantum

yield, and photoluminescence kinetics on the chemical structure. Whereas the exciton diffusion in the solid state determined by fluorescence depolarization and exciton-exciton annihilation is similar, the radiative and nonradiative decay rates notably change with the dendrons. A strong concentration quenching is observed in the neat films of the bisfluorene-cored dendrimers with carbazolyl and stilbenyl based dendrons and is modeled as energy transfer of the excitons to quenchers. Time-resolved fluorescence measurements were used as a tool for quantifying the concentration of quenchers in organic semiconductors. We found that one site per 370 dendrimers with carbazolyl dendrons and one site per 500 of those with stilbenyl dendrons act as a PL quencher. The most reasonable explanation for this quenching is the intermolecular hole transfer from the excited chromophore to the dendron in a face-to-face geometry. This result is particularly important for the design of blue light-emitting dendrimers with charge transporting dendrons. Our study demonstrates the critical role of the dendron chemical structure on the intermolecular interactions and the fluorescence properties of conjugated dendrimers, and shows that by a suitable choice of the dendron quenching in the solid state can be avoided, giving extremely high thin film PLQYs.

- <sup>1</sup>C. W. Tang and S. A. VanSlyke, *Appl. Phys. Lett.* **51**, 913 (1987).
- <sup>2</sup>J. H. Burroughes, D. D. C. Bradley, A. R. Brown, R. N. Marks, K. Mackay, R. H. Friend, P. L. Burn, and A. B. Holmes, *Nature (London)* **347**, 539 (1990).
- <sup>3</sup>M. A. Baldo, D. F. O'Brien, Y. You, A. Shoustikov, S. Sibley, M. E. Thompson, and S. R. Forrest, *Nature (London)* **395**, 151 (1998).
- <sup>4</sup>G. Yu, J. Gao, J. C. Hummelen, F. Wudl, and A. J. Heeger, *Science* **270**, 1789 (1995).
- <sup>5</sup>J. J. M. Halls, C. A. Walsh, N. C. Greenham, E. A. Marseglia, R. H. Friend, S. C. Moratti, and A. B. Holmes, *Nature (London)* **376**, 498 (1995).
- <sup>6</sup>A. R. Brown, A. Pomp, C. M. Hart, and D. M. De Leeuw, *Science* **270**, 972 (1995).
- <sup>7</sup>H. Sirringhaus, P. J. Brown, R. H. Friend, M. M. Nielsen, K. Bechgaard, B. M. W. Langeveld-Voss, A. J. H. Spiering, R. A. J. Janssen, E. W. Meijer, P. Herwig, and D. M. De Leeuw, *Nature (London)* **401**, 685 (1999).
- <sup>8</sup>I. D. W. Samuel, G. Rumbles, and C. J. Collison, *Phys. Rev. B* **52**, R11573 (1995).
- <sup>9</sup>T.-Q. Nguyen, V. Doan, and B. J. Schwartz, *J. Chem. Phys.* **110**, 4068 (1999).
- <sup>10</sup>T.-Q. Nguyen, I. B. Martini, J. Liu, and B. J. Schwartz, *J. Phys. Chem. B* **104**, 237 (2000).
- <sup>11</sup>J. Liu, Y. Shi, L. Ma, and Y. Yang, *J. Appl. Phys.* **88**, 605 (2000).
- <sup>12</sup>Y. Shi, J. Liu, and Y. Yang, *J. Appl. Phys.* **87**, 4254 (2000).
- <sup>13</sup>J. Liu, T. F. Guo, and Y. Yang, *J. Appl. Phys.* **91**, 1595 (2002).
- <sup>14</sup>A. J. Cadby, P. A. Lane, H. Mellor, S. J. Martin, M. Grell, C. Giebeler, D. D. C. Bradley, M. Wohlgenannt, C. An, and Z. V. Vardeny, *Phys. Rev. B* **62**, 15604 (2000).
- <sup>15</sup>I. D. W. Samuel, G. Rumbles, C. J. Collison, S. C. Moratti, and A. B. Holmes, *Chem. Phys.* **227**, 75 (1998).
- <sup>16</sup>W. J. Mitchell, P. L. Burn, R. K. Thomas, G. Fragnetto, J. P. J. Markham, and I. D. W. Samuel, *J. Appl. Phys.* **95**, 2391 (2004).
- <sup>17</sup>P. F. Miller, M. M. de Souza, S. C. Moratti, A. B. Holmes, I. D. W. Samuel, and G. Rumbles, *Polym. Int.* **55**, 784 (2006).
- <sup>18</sup>L. Rothberg, T. M. Jedju, P. D. Townsend, S. Etemad, and G. L. Baker, *Phys. Rev. Lett.* **65**, 100 (1990).
- <sup>19</sup>B. E. Kohler and I. D. W. Samuel, *J. Chem. Phys.* **103**, 6248 (1995).
- <sup>20</sup>P. Wood, I. D. W. Samuel, R. Schrock, and R. L. Christensen, *J. Chem. Phys.* **115**, 10955 (2001).
- <sup>21</sup>S. N. Yaliraki and R. J. Silbey, *J. Chem. Phys.* **104**, 1245 (1996).
- <sup>22</sup>J. M. Lupton, I. D. W. Samuel, R. Beavington, P. L. Burn, and H. Bässler, *Adv. Mater. (Weinheim, Ger.)* **13**, 258 (2001).
- <sup>23</sup>P. L. Burn, S. C. Lo, and I. D. W. Samuel, *Adv. Mater. (Weinheim, Ger.)*

- 19**, 1675 (2007).
- <sup>24</sup>M. E. Köse, W. J. Mitchell, N. Kopidakis, C. H. Chang, S. E. Shaheen, K. Kim, and G. Rumbles, *J. Am. Chem. Soc.* **129**, 14257 (2007).
- <sup>25</sup>S.-C. Lo, N. A. H. Male, J. P. J. Markham, S. W. Magennis, P. L. Burn, O. V. Salata, and I. D. W. Samuel, *Adv. Mater. (Weinheim, Ger.)* **14**, 975 (2002).
- <sup>26</sup>J. P. J. Markham, E. B. Namdas, T. D. Anthopoulos, I. D. W. Samuel, G. J. Richards, and P. L. Burn, *Appl. Phys. Lett.* **85**, 1463 (2004).
- <sup>27</sup>J. C. Ribierre, G. Tsiminis, S. Richardson, G. A. Turnbull, I. D. W. Samuel, H. S. Barcena, and P. L. Burn, *Appl. Phys. Lett.* **91**, 081108 (2007).
- <sup>28</sup>G. Tsiminis, J. C. Ribierre, A. Ruseckas, H. S. Barcena, G. J. Richards, P. L. Burn, and I. D. W. Samuel, *Adv. Mater. (Weinheim, Ger.)* (unpublished).
- <sup>29</sup>J. R. Lawrence, G. A. Turnbull, I. D. W. Samuel, G. J. Richards, and P. L. Burn, *Opt. Lett.* **29**, 869 (2004).
- <sup>30</sup>J. N. Demas, G. A. Crosby, *J. Phys. Chem.* **75**, 991 (1971).
- <sup>31</sup>N. C. Greenham, I. D. W. Samuel, G. R. Hayes, R. T. Phillips, R. R. Kessener, S. C. Moratti, A. B. Holmes, and R. H. Friend, *Chem. Phys. Lett.* **241**, 89 (1995).
- <sup>32</sup>J. D. Anderson, E. M. McDonald, P. A. Lee, M. L. Anderson, E. L. Ritchie, H. K. Hall, T. Hopkins, E. A. Mash, J. Wang, A. Padias, S. Thayumanavan, S. Barlow, S. R. Marder, G. E. Jabbour, S. Shaheen, B. Kippelen, N. Peyghambarian, R. M. Wightman, and N. R. Armstrong, *J. Am. Chem. Soc.* **120**, 9647 (1998).
- <sup>33</sup>R. Beavington, M. J. Frampton, J. M. Lupton, P. L. Burn, and I. D. W. Samuel, *Adv. Funct. Mater.* **13**, 211 (2003).
- <sup>34</sup>O. Varnavski, I. D. W. Samuel, L.-O. Palsson, R. Beavington, P. L. Burn, and T. Goodson III, *J. Chem. Phys.* **116**, 8893 (2002).
- <sup>35</sup>T. Förster, *Discuss. Faraday Soc.* **27**, 7 (1959).
- <sup>36</sup>M. Belletete, M. Ranger, S. Beaupre, M. Leclerc, and G. Durocher, *Chem. Phys. Lett.* **316**, 101 (2000).
- <sup>37</sup>K. A. Peterson, M. B. Zimmt, M. D. Fayer, Y. H. Jeng, and C. W. Frank, *Macromolecules* **22**, 874 (1989).
- <sup>38</sup>V. M. Agranovich and M. D. Galanin, *Electronic Excitation Energy Transfer in Condensed Matter* (North-Holland, Amsterdam, 1982).
- <sup>39</sup>M. A. Stevens, C. Silva, D. M. Russel, and R. H. Friend, *Phys. Rev. B* **63**, 165213 (2001).
- <sup>40</sup>E. B. Namdas, A. Ruseckas, I. D. W. Samuel, S.-C. Lo, and P. L. Burn, *Appl. Phys. Lett.* **86**, 091104 (2005).
- <sup>41</sup>A. J. Lewis, A. Ruseckas, O. P. M. Gaudin, G. R. Webster, P. L. Burn, and I. D. W. Samuel, *Org. Electron.* **7**, 452 (2006).
- <sup>42</sup>*Electronic Processes in Organic Crystals and Polymers*, edited by M. Pope and C. E. Swenberg, 2nd ed. (Oxford University Press, Oxford, 1999).
- <sup>43</sup>M. Tong, C.-X. Sheng, and Z. V. Vardeny, *Phys. Rev. B* **75**, 125207 (2007).